*Portugaliae Electrochimica Acta 24 (2006) 415-440*

**PORTUGALIAE ELECTROCHIMICA ACTA**

# The Use of Rotating Cylinder Electrode to Study the Effect of 1,3-Dihydroxypropane on Copper Electrorefining

**H.M.A. Soliman,**[a),*] **H.H. Abdel-Rahman**[b)]

[a)] *Institute of New Materials and Advanced Technologies, Mubarak City for Scientific Research and Technology Applications, New Borg El-Arab City, P.O. Box 21934 Alexandria, Egypt*
[b)] *Chemistry Department, Faculty of Science, Alexandria University, P.O. Box 426, Ibrahimia 21321, Alexandria, Egypt*

Received 24 July 2005; accepted 25 July 2006

**Abstract**

The effect of different concentrations of 1,3-dihydroxypropane (DHP) on the electrodeposition of copper powder from acidified copper sulphate solution has been studied at different temperatures and different speeds of rotation. Copper powder was electrodeposited onto rotating cylinder electrode (RCE) that made of pure copper. The inhibition percentage, P, in the electrodeposited copper powder was 0.00 – 92.91%, depending on the experimental variables. P was affected by temperature and mole fraction of DHP, while rotation did not show any influence whatsoever. Values of the activation energy of electrodeposition process, $E_a$, were found to be less than 28 k J $mol^{-1}$ indicating diffusion controlled process. The overall mass transfer correlations under the present conditions have been obtained using the dimensional analysis method. The data were valid for 80 < Sh (Sh = Sherwood number) < 3970, 290 < Sc (Sc = Schmidt number) < 59284 and 271 < Re (Re = Reynolds number) < 52705 and the results agreed with the previous studies of mass transfer to rotating cylinders in turbulent flow regimes. Experimental determination of the solution critical velocity was obtained for blank and 20% (v/v) DHP solutions at 298 K.

The effect of time, DHP content, temperature and the speed of rotation on the morphological changes of the electrodeposited copper powder as well as deposits composition and particle size have been studied. Various particle sizes ranged 60.5 – 203.4 nm were obtained, characterized by EDS and XRD and found to be pure copper with small amount of oxygen. Different topographs proved that the rate of copper electrodeposition increased by increasing time, temperature and the speed of rotation. In addition, they proved that the deposition rate decreased by adding DHP to the solution. Therefore, the results obtained by SEM supported those results obtained by electrochemical measurements. The morphological structure of deposited copper powder from 20% (v/v) DHP at 1000 rpm and 298 K was unique, rounded-crystalline aggregates with voids.

***Keywords:*** 1,3-dihydroxypropane, copper powder, electrodeposition, electrorefining, rotating cylinder electrode.

* Corresponding author. E-mail address: hsolman@link.net

## Introduction

The use of RCE, as a cathode reaction surface for metal electrodeposition or metal extraction, has proved successful for a wide range of applications [1]. The RCE provides high rates of mass transport due to high rates of convective-diffusion in turbulent flow [2] as stated by Eisenberg et al. [3], who found the relationship $Sh = 0.079\,Re^{0.7}\,Sc^{0.356}$ to hold for the range $100 < Re < 100{,}000$.

Copper is an intermediate metal [4], which has medium exchange current density ($10^{-5}$ to 1 mA $cm^{-2}$) and deposits at medium polarization. It deposits in very rough or powdery form when electrodeposition is carried out at the limiting current density. An addition agent is defined as any material, which is added to an electroplating bath for the specific purpose of modifying the physical properties of the deposit. Relatively small amounts of addition agent have large effect on the physical properties of deposits such as brightness, smoothness, hardness and ductility. Most addition agents are organic [5,6] compounds but, occasionally, inorganic [7] materials are employed. Organic solvents are also employed in the electrodeposition of metals that cannot be electrodeposited directly from aqueous solutions [8,9]. The importance of these media lies in the fact that changing their composition can vary their physicochemical properties. Bright copper has been electrodeposited from aqueous ammonia [10] solutions. Electrodeposition of copper has been studied in presence of ethanol, n-propanol, iso-propanol and tert-butanol [11] and methanol, ethylene glycol and glycerol [12]. Electrodeposition of nickel from mixed baths [13] and from nonaqueous baths [14] led to some promising results. In the case of mixed solvent bath, the change in physicochemical properties of the deposit is attributed to the change in solvent composition. Moreover, the effect of aprotic constituent, dielectric constant and state of solvation of ions to be electrodeposited can easily vary by simply changing the composition of the mixed solvents. During electrodeposition studies of copper and nickel from water-methanol [15] bath, the change in electronic state of metal ion was attributed to the structural changes of solvent.

Compromising between the mass production and particle size is a challenging task in the industry of metallic powders and, given that, the microstructure and morphology of the electrodeposited metal are affected by the state of solvation; therefore, this work aims to investigate copper powder electrodeposition from acidified solutions of copper sulphate mixed with different contents of DHP under forced convection regime. Such investigation included change in temperature, rotation speed of RCE, and concentration of DHP. In addition, it aims to study the SEM topographs and EDS analysis to support the experimental measurements and to shed more light on copper powder production. Overall, this study is concerned with all possibilities to generate new ideas for understanding and prediction of the electrode and cell geometries through dimensionless correlations to reach the optimum conditions useful in the industry of copper powder.

## Experimental Techniques

All chemicals were Analar grade and supplied by BDH chemicals Ltd. Solutions were prepared with water of resistivity 15 MΩ cm, which was obtained from a MilliRo/ MilliQ water purification system. Copper sulphate concentration and content were checked by the iodine-thiosulphate method [11]. The density and viscosity for all solutions, Table 1, were measured at 298, 303, 308 and 313 K [11].

**Table 1**. Viscosities and densities for all solutions at different temperatures.

| | Temperature (T), K | Viscosity ($\eta$), poise | Density, ($\rho$), g cm$^{-3}$ |
|---|---|---|---|
| Blank, 0% (v/v) DHP | 298 | 0.01084 | 1.09928 |
| | 303 | 0.00972 | 1.09647 |
| | 308 | 0.00879 | 1.09365 |
| | 313 | 0.00800 | 1.09084 |
| 10% (v/v) DHP | 298 | 0.01129 | 1.10656 |
| | 303 | 0.01013 | 1.10373 |
| | 308 | 0.00915 | 1.10090 |
| | 313 | 0.00833 | 1.09807 |
| 20% (v/v) DHP | 298 | 0.01304 | 1.11484 |
| | 303 | 0.01169 | 1.11199 |
| | 308 | 0.01056 | 1.10913 |
| | 313 | 0.00961 | 1.10628 |
| 30% (v/v) DHP | 298 | 0.01543 | 1.12810 |
| | 303 | 0.01384 | 1.12522 |
| | 308 | 0.01250 | 1.12233 |
| | 313 | 0.01138 | 1.11945 |
| 40% (v/v) DHP | 298 | 0.01879 | 1.13638 |
| | 303 | 0.01685 | 1.13348 |
| | 308 | 0.01523 | 1.13057 |
| | 313 | 0.01386 | 1.12766 |
| 50% (v/v) DHP | 298 | 0.02334 | 1.14865 |
| | 303 | 0.02093 | 1.14571 |
| | 308 | 0.01892 | 1.14277 |
| | 313 | 0.01721 | 1.13984 |
| 60% (v/v) DHP | 298 | 0.02964 | 1.15793 |
| | 303 | 0.02658 | 1.15497 |
| | 308 | 0.02402 | 1.15200 |
| | 313 | 0.02186 | 1.14904 |

A standard glass type cell [16] with a polypropylene lid was used in all experiments. The solution volume was 1000 mL. The polypropylene lid contained four inlets, which were used for working electrode WE immersion, luggin probe (reference electrode RE: saturated calomel electrode, SCE), counter electrode CE (copper) and thermometer to measure the temperature.

A 99.99% purity copper cylindrical sample was used as WE. This sample was rotated at controlled rates by an analytical rotator model A.S.R. made by PINE Instrument Company. The cylindrical samples of copper had dimensions of 8 mm height and 12 mm diameter. The specimens were lightly abraded with 1200 grade silicon carbide paper, washed with distilled water, acetone and deionised water and dried in a cool air stream prior to use. The anode CE, was machined

from high purity (99.99%), commercially available copper. In order to ensure a correct control of the specimen rotation rate and the correct recording of potentials, regular checking of the rotation rate was carried out.
The potentiostat was Ministat Precision Potentiostat made by Thompson Electrochem Ltd. coupled to a Chemical Electronics (Birtley) Ltd. Sweep Generator and controlled by an 8086 Personal Computer via an Advantech PCL-718 Lab Card and a PCLD-780 wiring terminal board. In this system the Advantech Labtech Aquire software was used.
All electrochemical experiments and polarization curves were carried out using a potentiodynamic method. The sweep rate in all experiments was 100 mV s, which considered being suitable for copper electrodeposition [4].

*Cathodic polarization*
The variables used in this investigation were rotation speed (0 – 1000 rpm), temperature (298 – 313 K), and blank solution (0.1 M $CuSO_4$ and 1.5 M $H_2SO_4$) without and with DHP 10 - 60 % (v/v) with a polarisation potential range of 700 mV.

*Determination of the critical velocity*
In these experiments, cathodic polarisation was used. The temperature was 298 K in all experiments and additive's concentration was 20% (v/v) DHP besides the blank solution. The rotation range was 1500 to 7000 rpm. The experimental procedure and set up were similar to cathodic polarisation.

*Morphology and composition analyses*
An AMRAY 1810 Scanning Electron Microscope (SEM) was used to examine the surface topography of specimens after experiment, while Energy Dispersive X-Ray Analysis (EDS) was used for elemental analyses. The specimens were examined through an acceleration potential of 20 KeV; the specimens were coated with carbon to avoid electron charging of the surface since the surface film may not be electrically conductive.
Two types of specimens were prepared to examine the surface topography. The first type of specimens was used for free convection experiments, while the second type was used for forced convection ones. The free convection specimens were made of copper rods that were cut into small pieces of dimensions 0.8 cm height and 1.2 cm diameter; while those used for forced convection were made of copper cylinders with 0.8 cm in height and 1.2 cm in diameter. For all specimens, the surfaces for SEM analyses were polished with series of silicon carbide paper grades in the range 120 – 1200 μm, then with 3 μm diamond paste followed by 1 μm diamond paste on a polishing wheel. After washing with deionised water and degreasing in acetone, warm air was blown over the surface. These specimens were stored in a desiccator over silica gel prior to use.
X-ray diffraction (XRD) measurement for copper powder was carried out using a Shimazu XRD-7000 X-Ray Diffractometer with Cu-Ka1 radiation operated at 40 kV and 30 mA, with a scan speed of $2\theta$ $min^{-1}$.

Temperature: 298 – 313 K, DHP content: 0 – 60% (v/v), rotation rate: 0 - 1000 rpm, and time: 10 - 30 minutes, were the different variables that have been employed to study the surface analysis by EDS and XRD identification measurements.

## Results and discussion

*Cathodic polarisation*

Values of the limiting current densities for all solutions at different rotations and different temperatures using copper anode are given in Table 2. Noticeably, the limiting current density decreases with increasing DHP mole fraction and increases by increasing temperature. The increase of mass transport under forced or turbulent conditions may refer to [2] elevation in solution temperature, roughness of the deposit and/or the increase in agitation. Eq. 1 was used to calculate the mass transfer coefficients, k, for DHP solutions.

$$k = \frac{i_l}{nFC_\circ} \tag{1}$$

where: n = number of electrons involved in the reaction, F = Faraday constant = 96500 (C $mol^{-1}$, C = A s), $C_\circ$ = bulk concentration of copper sulphate (mol $cm^{-3}$).

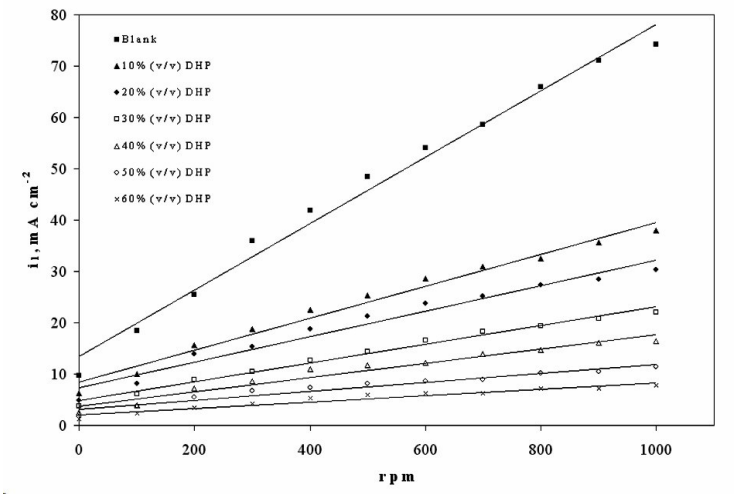


**Figure 1**. Variation of limiting current density, $i_l$, with the speed of rotation, rpm, at 298 K.

**Table 2**. Values of the limiting current density ($i_l$), mA $cm^{-2}$ for all solutions at different temperatures and at different speeds of rotation.

| | rpm | 298 K | 303 K | 308 K | 313 K |
|---|---|---|---|---|---|
| Blank, 0% (v/v) DHP | 0 | 9.70 | 10.80 | 11.76 | 12.93 |
| | 100 | 18.51 | 26.01 | 30.82 | 33.78 |
| | 200 | 25.41 | 35.73 | 37.01 | 54.00 |
| | 300 | 35.88 | 45.52 | 55.40 | 66.77 |
| | 400 | 41.89 | 53.51 | 61.62 | 74.48 |
| | 500 | 48.51 | 60.88 | 64.67 | 84.45 |
| | 600 | 54.12 | 71.92 | 80.61 | 99.41 |
| | 700 | 58.63 | 73.78 | 96.56 | 109.97 |
| | 800 | 65.92 | 82.96 | 98.05 | 118.30 |
| | 900 | 71.07 | 87.87 | 111.13 | 125.64 |
| | 1000 | 74.27 | 96.34 | 112.74 | 135.79 |
| 10% (v/v) DHP | 0 | 6.32 | 6.92 | 7.27 | 7.99 |
| | 100 | 9.93 | 11.95 | 13.16 | 15.50 |
| | 200 | 15.68 | 18.12 | 19.36 | 22.29 |
| | 300 | 18.69 | 21.98 | 24.90 | 27.97 |
| | 400 | 22.57 | 26.97 | 29.52 | 34.48 |
| | 500 | 25.34 | 30.97 | 34.52 | 39.06 |
| | 600 | 28.55 | 33.69 | 37.68 | 43.23 |
| | 700 | 30.86 | 36.89 | 41.71 | 46.43 |
| | 800 | 32.57 | 40.58 | 45.16 | 51.26 |
| | 900 | 35.68 | 43.16 | 48.57 | 55.08 |
| | 1000 | 38.02 | 46.05 | 51.33 | 59.76 |
| 20% (v/v) DHP | 0 | 4.82 | 5.08 | 5.75 | 6.09 |
| | 100 | 8.13 | 8.89 | 10.13 | 11.03 |
| | 200 | 13.94 | 14.44 | 15.65 | 16.79 |
| | 300 | 15.31 | 16.48 | 18.59 | 21.17 |
| | 400 | 18.72 | 19.26 | 22.07 | 25.11 |
| | 500 | 21.20 | 24.34 | 26.55 | 29.46 |
| | 600 | 23.77 | 26.18 | 29.12 | 32.27 |
| | 700 | 25.21 | 29.59 | 32.00 | 36.91 |
| | 800 | 27.38 | 30.53 | 34.27 | 40.39 |
| | 900 | 28.45 | 33.07 | 37.58 | 47.38 |
| | 1000 | 30.33 | 34.54 | 39.49 | 47.71 |
| 30% (v/v) DHP | 0 | 3.76 | 3.89 | 4.10 | 4.49 |
| | 100 | 6.13 | 6.27 | 6.48 | 8.17 |
| | 200 | 8.85 | 9.85 | 12.26 | 13.63 |
| | 300 | 10.44 | 13.64 | 13.85 | 16.61 |
| | 400 | 12.68 | 16.40 | 17.05 | 19.38 |
| | 500 | 14.40 | 17.33 | 19.57 | 22.78 |
| | 600 | 16.50 | 19.12 | 22.15 | 26.49 |
| | 700 | 18.33 | 21.05 | 23.94 | 27.58 |
| | 800 | 19.36 | 23.39 | 26.28 | 30.66 |
| | 900 | 20.77 | 24.22 | 27.66 | 32.70 |
| | 1000 | 22.08 | 26.35 | 29.42 | 34.59 |
| 40% (v/v) DHP | 0 | 2.56 | 2.59 | 2.80 | 3.12 |
| | 100 | 3.89 | 5.75 | 6.20 | 6.73 |
| | 200 | 7.11 | 7.64 | 9.18 | 10.51 |
| | 300 | 8.62 | 9.39 | 10.79 | 12.62 |
| | 400 | 10.93 | 12.27 | 12.93 | 14.58 |
| | 500 | 11.74 | 12.79 | 14.44 | 17.14 |
| | 600 | 12.27 | 14.33 | 16.05 | 18.71 |
| | 700 | 13.91 | 15.80 | 17.45 | 20.78 |
| | 800 | 14.61 | 17.00 | 20.50 | 23.83 |
| | 900 | 16.09 | 18.26 | 22.67 | 25.62 |
| | 1000 | 16.44 | 18.78 | 23.65 | 27.68 |
| 50% (v/v) DHP | 0 | 1.65 | 1.72 | 1.84 | 2.13 |
| | 100 | 3.68 | 4.17 | 4.91 | 5.74 |
| | 200 | 5.47 | 5.50 | 7.51 | 8.34 |
| | 300 | 6.73 | 7.67 | 9.60 | 10.29 |
| | 400 | 7.32 | 8.06 | 10.50 | 11.59 |
| | 500 | 8.20 | 8.76 | 10.54 | 11.87 |
| | 600 | 8.59 | 9.81 | 12.27 | 14.91 |
| | 700 | 8.90 | 10.76 | 13.64 | 17.22 |
| | 800 | 10.13 | 11.63 | 15.27 | 20.03 |
| | 900 | 10.51 | 12.72 | 16.42 | 20.93 |
| | 1000 | 11.35 | 13.46 | 16.46 | 23.89 |
| 60% (v/v) DHP | 0 | 1.23 | 1.23 | 1.30 | 1.40 |
| | 100 | 2.35 | 2.56 | 2.78 | 2.80 |
| | 200 | 3.45 | 3.65 | 3.72 | 3.83 |
| | 300 | 4.23 | 4.35 | 5.53 | 5.77 |
| | 400 | 5.27 | 5.43 | 6.24 | 6.86 |
| | 500 | 5.97 | 6.17 | 6.93 | 8.67 |
| | 600 | 6.21 | 6.62 | 8.15 | 11.19 |
| | 700 | 6.21 | 8.39 | 10.17 | 11.77 |
| | 800 | 7.11 | 8.53 | 10.54 | 12.35 |
| | 900 | 7.18 | 9.55 | 12.62 | 14.13 |
| | 1000 | 7.76 | 11.40 | 13.44 | 14.84 |

**Table 3**. Values of the percentage of inhibition (P) for all solutions at different temperatures and different speeds of rotation.

| | rpm | 298 K | 303 K | 308 K | 313 K |
|---|---|---|---|---|---|
| 10% (v/v) DHP | 0 | 34.82 | 35.89 | 38.20 | 38.18 |
| | 100 | 46.34 | 54.04 | 57.31 | 54.11 |
| | 200 | 38.29 | 49.29 | 47.70 | 58.73 |
| | 300 | 47.91 | 51.72 | 55.04 | 58.11 |
| | 400 | 46.12 | 49.59 | 52.09 | 53.71 |
| | 500 | 47.75 | 49.14 | 46.62 | 53.75 |
| | 600 | 47.24 | 53.16 | 53.25 | 56.51 |
| | 700 | 47.36 | 50.00 | 56.80 | 57.78 |
| | 800 | 50.59 | 51.09 | 53.94 | 56.67 |
| | 900 | 49.80 | 50.88 | 56.29 | 56.16 |
| | 1000 | 48.81 | 52.20 | 54.48 | 55.99 |
| 20% (v/v) DHP | 0 | 50.34 | 52.94 | 51.10 | 52.93 |
| | 100 | 56.10 | 65.80 | 67.13 | 67.34 |
| | 200 | 45.13 | 59.58 | 57.72 | 68.92 |
| | 300 | 57.32 | 63.79 | 66.44 | 68.30 |
| | 400 | 55.30 | 64.01 | 64.18 | 66.29 |
| | 500 | 56.30 | 60.02 | 58.95 | 65.12 |
| | 600 | 56.07 | 63.60 | 63.87 | 67.54 |
| | 700 | 57.00 | 59.89 | 66.86 | 66.43 |
| | 800 | 58.46 | 63.20 | 65.05 | 65.86 |
| | 900 | 59.96 | 62.37 | 66.18 | 62.29 |
| | 1000 | 59.17 | 64.15 | 64.98 | 64.86 |
| 30% (v/v) DHP | 0 | 61.27 | 63.96 | 65.14 | 65.30 |
| | 100 | 66.87 | 75.89 | 78.99 | 75.83 |
| | 200 | 65.16 | 72.43 | 66.87 | 74.76 |
| | 300 | 70.91 | 70.03 | 75.00 | 75.12 |
| | 400 | 69.74 | 69.36 | 72.33 | 73.98 |
| | 500 | 70.32 | 71.54 | 69.74 | 73.03 |
| | 600 | 69.51 | 73.42 | 72.52 | 73.35 |
| | 700 | 68.74 | 71.47 | 75.21 | 74.92 |
| | 800 | 70.63 | 71.81 | 73.20 | 74.08 |
| | 900 | 70.77 | 72.44 | 75.11 | 73.98 |
| | 1000 | 70.27 | 72.65 | 73.91 | 74.53 |
| 40% (v/v) DHP | 0 | 73.62 | 75.99 | 76.16 | 75.87 |
| | 100 | 78.98 | 77.90 | 79.88 | 80.08 |
| | 200 | 72.00 | 78.62 | 75.19 | 80.53 |
| | 300 | 75.98 | 79.37 | 80.52 | 81.10 |
| | 400 | 73.90 | 77.08 | 79.01 | 80.43 |
| | 500 | 75.80 | 78.99 | 77.67 | 79.71 |
| | 600 | 77.34 | 80.07 | 80.09 | 81.18 |
| | 700 | 76.27 | 78.58 | 81.93 | 81.10 |
| | 800 | 77.83 | 79.51 | 79.09 | 79.86 |
| | 900 | 77.37 | 79.22 | 79.60 | 79.61 |
| | 1000 | 77.87 | 80.50 | 79.02 | 79.61 |
| 50% (v/v) DHP | 0 | 83.01 | 84.10 | 84.35 | 83.53 |
| | 100 | 80.11 | 83.97 | 84.08 | 83.01 |
| | 200 | 78.48 | 84.60 | 79.72 | 84.56 |
| | 300 | 81.25 | 83.14 | 82.67 | 84.59 |
| | 400 | 82.52 | 84.94 | 82.96 | 84.45 |
| | 500 | 83.09 | 85.61 | 83.70 | 85.94 |
| | 600 | 84.13 | 86.36 | 84.78 | 85.01 |
| | 700 | 84.82 | 85.42 | 85.87 | 84.35 |
| | 800 | 84.64 | 85.98 | 84.43 | 83.07 |
| | 900 | 85.21 | 85.52 | 85.22 | 83.34 |
| | 1000 | 84.71 | 86.03 | 85.40 | 82.41 |
| 60% (v/v) DHP | 0 | 87.34 | 88.63 | 88.95 | 89.18 |
| | 100 | 87.32 | 90.16 | 90.98 | 91.72 |
| | 200 | 86.44 | 89.78 | 89.95 | 92.91 |
| | 300 | 88.21 | 90.44 | 90.02 | 91.36 |
| | 400 | 87.42 | 89.86 | 89.87 | 90.79 |
| | 500 | 87.69 | 89.86 | 89.29 | 89.74 |
| | 600 | 88.53 | 90.80 | 89.88 | 88.74 |
| | 700 | 89.41 | 88.62 | 89.47 | 89.30 |
| | 800 | 89.21 | 89.72 | 89.25 | 89.56 |
| | 900 | 89.89 | 89.13 | 88.64 | 88.76 |
| | 1000 | 89.55 | 88.17 | 88.08 | 89.07 |

It is clear in Table 2 and in Fig. 1 that the limiting current density increases with increasing the speed of rotation, which proves that the electrodeposition process of copper in presence of DHP as well as in aqueous media is diffusion-controlled reaction.

The percentage of inhibition, P, was calculated from Eq. 2. P caused by DHP was in the range of 0.00 - 92.91% depending on the concentration of DHP as well as on the temperature.

$$P = \frac{i_{l_{blank}} - i_{l_{DHP.}}}{i_{l_{blank}}} X100 \qquad (2)$$

Table 3 gives the values of P, which shows that P increased as the mole fraction of DHP, X, increased, but it was not affected by rotation. This indicates that the rotation factor has little effect on the adsorption process and the decrease in mass transfer coefficient in this case is attributable to the increase in the interfacial viscosity [16], which is caused by the adsorption of alcohol molecules at the cylinder surface with their non-polar ends, while the polar ones are directed towards solution.

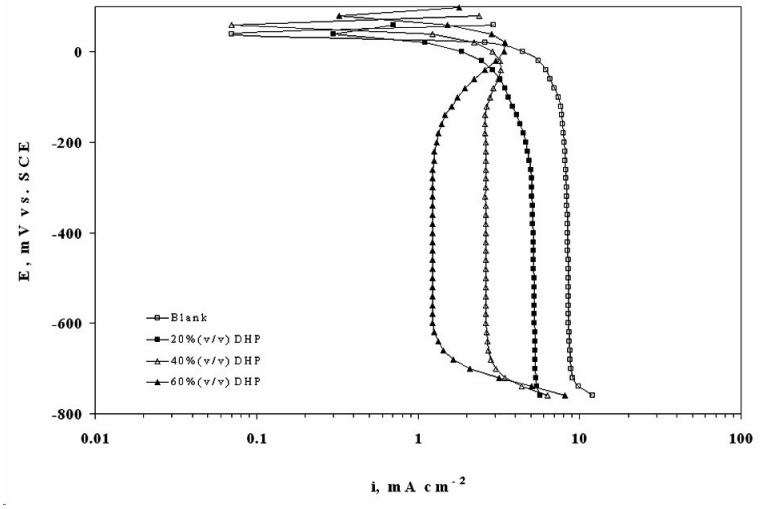


**Figure 2**. Typical potential-current curves obtained at 298 K, no rotation, and different DHP contents.

Fig. 2 shows the cathodic polarisation curves for copper powder that electrodeposited from acid-sulphate solution with variable amounts of DHP at 298 K and zero rpm as an example. It is obvious that in alcohol-free solution the current at the beginning increases linearly, then as the cathodic potential increases it tends to exhibit limiting current plateau. The reduction of copper ions takes place through two steps [17]:

$$\text{Step}^1 : Cu^{2+} + e \xleftrightarrow{\text{Slow}} Cu^{+} ; \text{Step}^2 : Cu^{+} + e \xleftrightarrow{\text{Fast}} Cu$$

It was assumed that the first step in this process occurred slowly and the rate was controlled by the equilibrium between $Cu^{2+}$ and $Cu^{+}$ at the electrode surface. However, addition of alcohol to the sulphate solution increases the cathodic polarisation and decreases the value of the limiting current density. The observed changes in the cathodic polarisation in the presence of DHP suggest that it acts as an inhibitor, which is confirmed by the observation, at any given overpotential, the current density for copper deposition from solutions containing DHP is always lower than that for the blank solution. This inhibition effect may be due to the adsorption of alcohol molecules on the cathode surface and/or the

complexation of $Cu^{2+}$ with alcohol molecules. It is known that in acidic media, $Cu^{2+}$ can complex with alcohol molecules via the alcohol hydroxyl groups and exists as a cationic complex [17].

*Adsorption isotherms*

Adsorption isotherms are very important in determining the mechanism of organo-electrochemical reactions. The most frequently used isotherms are those of Langmuir, Frumkin, Parsons, Temkin, Flory-Huggins and Bockris-Swinkels. All these isotherms are of the general form:

$$f(\theta, x)\exp(-a\theta) = K_e\, C \tag{3}$$

where $\theta$ is the surface coverage, $K_e$ is the equilibrium constant, C is the concentration of the electrolyte and $f(\theta,x)$ is the configurational factor that depends essentially on the physical model and assumptions underlying the derivation of the isotherm. The mechanism of electrodeposition inhibition is generally believed to be due to the formation and maintenance of an adsorbed film on the metal surface.

The surface coverage, $\theta$, can be determined using the following equation:

$$\theta = 1 - \frac{i_{DHP}}{i_{Blank}} \tag{4}$$

where $i_{DHP}$ and $i_{Blank}$ are the limiting current densities in case of solvent and blank solutions, respectively.

Values of the equilibrium constant were computed and listed in Table 4 using Langmuir isotherm:

$$K_e\, C = \frac{\theta}{1-\theta} \tag{5}$$

**Table 4**. Values of the equilibrium constant of adsorption ($K_e$) of DHP on copper at different temperatures and different speeds of rotation.

| rpm | 298 K | 303 K | 308 K | 313 K |
|---|---|---|---|---|
| 0 | 0.27 | 0.29 | 0.30 | 0.31 |
| 100 | 0.49 | 0.73 | 0.84 | 0.72 |
| 200 | 0.31 | 0.54 | 0.50 | 0.81 |
| 300 | 0.53 | 0.61 | 0.77 | 0.83 |
| 400 | 0.48 | 0.57 | 0.65 | 0.69 |
| 500 | 0.51 | 0.52 | 0.49 | 0.68 |
| 600 | 0.48 | 0.63 | 0.66 | 0.83 |
| 700 | 0.47 | 0.56 | 0.81 | 0.85 |
| 800 | 0.55 | 0.60 | 0.71 | 0.81 |
| 900 | 0.54 | 0.60 | 0.81 | 0.76 |
| 1000 | 0.52 | 0.66 | 0.75 | 0.80 |

When $\log \frac{\theta}{1-\theta}$ was plotted versus log C, straight lines were obtained with slopes nearly equal unity, which proves the fact that the adsorption of DHP on copper surface obeys the Langmuir adsorption isotherm. As a result, this leads to the suggestion that the adsorbed molecules don't interact with each other. In addition, straight lines were obtained when θ was plotted versus log C at different temperatures, indicating that the adsorption of DHP on copper surface follows Temkin's adsorption isotherm as well.

The free energy of adsorption, $\Delta G_{ads}$, at different temperatures was calculated and listed in Table 5 using the following equation:

$$K_e = \frac{1}{55.5} \exp[\frac{-\Delta G_{ads}}{RT}] \quad (6)$$

The value of 55.5 is the concentration of water in solution expressed in mol $L^{-1}$. The negative sign of $\Delta G_{ads}$ values indicates the spontaneous adsorption of DHP molecules, which is usually characteristic for strong interaction with metal surface. From Table 5, values of $\Delta G_{ads}$ are more positive than -40 k J $mol^{-1}$, indicating physical adsorption on metal surface.

*Thermodynamic treatment of the results*

To investigate the mechanism of the electrodeposition process, the activation energies, $E_a$, of the process were calculated from the values of the limiting current density in absence and in presence of DHP at different temperatures according to Arrhenius equation:

$$\ln(i_l) = \ln(A) - \frac{E_a}{R}\frac{1}{T} \quad (7)$$

where A is a pre-exponential factor related to concentration, steric effects, metal surface characteristics, etc; R is the molar gas constant and T is the absolute temperature.

**Table 5**. Values of free energy of adsorption ($\Delta G_{ads}$) for DHP on copper at different temperatures and different speeds of rotation.

| Solution | rpm | $-\Delta G_{ads}$, k J mol$^{-1}$ | | | |
|---|---|---|---|---|---|
| | | 298 K | 303 K | 308 K | 313 K |
| Blank, 0 % (v/v) DHP | 0 | 9.20 | 9.47 | 9.88 | 10.04 |
| 10 % (v/v) DHP | | 12.51 | 12.98 | 13.00 | 13.41 |
| 20 % (v/v) DHP | | 14.61 | 15.15 | 15.53 | 15.80 |
| 30 % (v/v) DHP | | 16.73 | 17.33 | 17.64 | 17.89 |
| 40 % (v/v) DHP | | 18.67 | 19.19 | 19.55 | 19.71 |
| 50 % (v/v) DHP | | 19.98 | 20.62 | 21.05 | 21.45 |
| 60 % (v/v) DHP | | 10.39 | 11.34 | 11.87 | 11.73 |
| Blank, 0 % (v/v) DHP | 100 | 13.08 | 14.33 | 14.72 | 14.98 |
| 10 % (v/v) DHP | | 15.22 | 16.59 | 17.32 | 17.13 |
| 20 % (v/v) DHP | | 17.47 | 17.60 | 18.20 | 18.53 |
| 30 % (v/v) DHP | | 18.20 | 19.16 | 19.50 | 19.61 |
| 40 % (v/v) DHP | | 19.98 | 21.03 | 21.62 | 22.22 |
| 50 % (v/v) DHP | | 9.57 | 10.86 | 10.88 | 12.22 |
| 60 % (v/v) DHP | | 11.99 | 13.66 | 13.69 | 15.17 |
| Blank, 0 % (v/v) DHP | 200 | 15.03 | 16.14 | 15.73 | 16.98 |
| 10 % (v/v) DHP | | 16.53 | 17.71 | 17.51 | 18.60 |
| 20 % (v/v) DHP | | 17.95 | 19.28 | 18.74 | 19.91 |
| 30 % (v/v) DHP | | 19.78 | 20.92 | 21.32 | 22.66 |
| 40 % (v/v) DHP | | 10.55 | 11.11 | 11.64 | 12.15 |
| 50 % (v/v) DHP | | 13.20 | 14.11 | 14.64 | 15.10 |
| 60 % (v/v) DHP | | 15.69 | 15.84 | 16.74 | 17.03 |
| Blank, 0 % (v/v) DHP | 300 | 17.04 | 17.82 | 18.30 | 18.70 |
| 10 % (v/v) DHP | | 18.38 | 19.01 | 19.24 | 19.92 |
| 20 % (v/v) DHP | | 20.18 | 21.11 | 21.34 | 22.10 |
| 30 % (v/v) DHP | | 10.37 | 10.90 | 11.33 | 11.68 |
| 40 % (v/v) DHP | | 13.00 | 14.13 | 14.39 | 14.86 |
| 50 % (v/v) DHP | | 15.55 | 15.76 | 16.39 | 16.88 |
| 60 % (v/v) DHP | | 16.77 | 17.48 | 18.06 | 18.58 |
| Blank, 0 % (v/v) DHP | 400 | 18.59 | 19.35 | 19.29 | 19.89 |
| 10 % (v/v) DHP | | 20.00 | 20.95 | 21.29 | 21.92 |
| 20 % (v/v) DHP | | 10.53 | 10.85 | 10.77 | 11.69 |
| 30 % (v/v) DHP | | 13.10 | 13.71 | 13.82 | 14.73 |
| 40 % (v/v) DHP | | 15.61 | 16.03 | 16.07 | 16.75 |
| 50 % (v/v) DHP | | 17.02 | 17.76 | 17.86 | 18.47 |
| 60 % (v/v) DHP | | 18.69 | 19.48 | 19.43 | 20.20 |
| Blank, 0 % (v/v) DHP | 500 | 20.06 | 20.95 | 21.14 | 21.60 |
| 10 % (v/v) DHP | | 10.48 | 11.26 | 11.45 | 11.98 |
| 20 % (v/v) DHP | | 13.08 | 14.09 | 14.35 | 15.01 |
| 30 % (v/v) DHP | | 15.52 | 16.26 | 16.42 | 16.79 |
| 40 % (v/v) DHP | | 17.23 | 17.93 | 18.23 | 18.71 |
| 50 % (v/v) DHP | | 18.88 | 19.64 | 19.64 | 20.00 |
| 60 % (v/v) DHP | | 20.26 | 21.22 | 21.30 | 21.33 |
| Blank, 0 % (v/v) DHP | 600 | 10.49 | 10.94 | 11.82 | 12.11 |
| 10 % (v/v) DHP | | 13.17 | 13.69 | 14.69 | 14.88 |
| 20 % (v/v) DHP | | 15.43 | 16.02 | 16.77 | 17.00 |
| 30 % (v/v) DHP | | 17.08 | 17.70 | 18.54 | 18.70 |
| 40 % (v/v) DHP | | 19.01 | 19.44 | 19.86 | 19.87 |
| 50 % (v/v) DHP | | 20.48 | 20.62 | 21.18 | 21.48 |
| 60 % (v/v) DHP | | 10.81 | 11.05 | 11.52 | 12.00 |
| Blank, 0 % (v/v) DHP | 700 | 13.32 | 14.04 | 14.48 | 14.81 |
| 10 % (v/v) DHP | | 15.65 | 16.06 | 16.50 | 16.89 |
| 20 % (v/v) DHP | | 17.30 | 17.84 | 18.07 | 18.49 |
| 30 % (v/v) DHP | | 18.97 | 19.56 | 19.57 | 19.62 |
| 40 % (v/v) DHP | | 20.43 | 20.91 | 21.12 | 21.55 |
| 50 % (v/v) DHP | | 10.74 | 11.02 | 11.76 | 11.94 |
| 60 % (v/v) DHP | | 13.47 | 13.95 | 14.61 | 14.41 |
| Blank, 0 % (v/v) DHP | 800 | 15.67 | 16.14 | 16.76 | 16.87 |
| 10 % (v/v) DHP | | 17.24 | 17.80 | 18.15 | 18.45 |
| 20 % (v/v) DHP | | 19.08 | 19.47 | 19.73 | 19.67 |
| 30 % (v/v) DHP | | 20.61 | 20.75 | 20.97 | 21.34 |
| 40 % (v/v) DHP | | 10.64 | 11.16 | 11.58 | 11.92 |
| 50 % (v/v) DHP | | 13.39 | 14.15 | 14.47 | 14.70 |
| 60 % (v/v) DHP | | 15.61 | 16.16 | 16.60 | 16.95 |
| Blank, 0 % (v/v) DHP | 900 | 17.31 | 18.00 | 18.06 | 18.45 |
| 10 % (v/v) DHP | | 18.99 | 19.57 | 19.76 | 19.50 |
| 20 % (v/v) DHP | | 20.52 | 20.51 | 20.83 | 21.42 |
| 30 % (v/v) DHP | | 9.20 | 9.47 | 9.88 | 10.04 |
| 40 % (v/v) DHP | | 12.51 | 12.98 | 13.00 | 13.41 |
| 50 % (v/v) DHP | | 14.61 | 15.15 | 15.53 | 15.80 |
| 60 % (v/v) DHP | | 16.73 | 17.33 | 17.64 | 17.89 |
| Blank, 0 % (v/v) DHP | 1000 | 18.67 | 19.19 | 19.55 | 19.71 |
| 10 % (v/v) DHP | | 19.98 | 20.62 | 21.05 | 21.45 |
| 20 % (v/v) DHP | | 10.39 | 11.34 | 11.87 | 11.73 |
| 30 % (v/v) DHP | | 13.08 | 14.33 | 14.72 | 14.98 |
| 40 % (v/v) DHP | | 15.22 | 16.59 | 17.32 | 17.13 |
| 50 % (v/v) DHP | | 17.47 | 17.60 | 18.20 | 18.53 |
| 60 % (v/v) DHP | | 18.20 | 19.16 | 19.50 | 19.61 |

**Table 6**. Electrodeposition average thermodynamic parameters within the temperature range 298 – 313 K for DHP solutions at different speeds of rotation.

| | rpm | $E_a$, k J mol$^{-1}$ | $\Delta H^*$, k J mol$^{-1}$ | $\Delta S^*$, J mol$^{-1}$ K$^{-1}$ | $\Delta G^*$, k J mol$^{-1}$ |
|---|---|---|---|---|---|
| Blank, 0% (v/v) DHP | 0 | 14.7 | 12.2 | -185.1 | 68.7 |
| 10% (v/v) DHP | | 11.7 | 9.0 | -198.9 | 69.9 |
| 20% (v/v) DHP | | 12.8 | 8.9 | -197.5 | 70.6 |
| 30% (v/v) DHP | | 9.1 | 7.3 | -212.2 | 71.3 |
| 40% (v/v) DHP | | 10.4 | 8.6 | -211.0 | 72.3 |
| 50% (v/v) DHP | | 13.0 | 8.6 | -206.0 | 73.4 |
| 60% (v/v) DHP | | 6.9 | 6.9 | -228.6 | 74.2 |
| Blank, 0% (v/v) DHP | 100 | 27.9 | 25.4 | -134.7 | 66.5 |
| 10% (v/v) DHP | | 22.2 | 18.5 | -159.7 | 68.5 |
| 20% (v/v) DHP | | 16.3 | 25.4 | -181.5 | 69.2 |
| 30% (v/v) DHP | | 13.7 | 13.3 | -192.6 | 70.0 |
| 40% (v/v) DHP | | 26.8 | 14.8 | -151.4 | 70.5 |
| 50% (v/v) DHP | | 23.2 | 12.6 | -164.9 | 71.0 |
| 60% (v/v) DHP | | 9.5 | 2.8 | -214.3 | 72.4 |
| Blank, 0% (v/v) DHP | 200 | 31.8 | 29.3 | -119.1 | 65.7 |
| 10% (v/v) DHP | | 17.4 | 16.5 | -172.2 | 67.4 |
| 20% (v/v) DHP | | 9.9 | 19.6 | -198.6 | 68.0 |
| 30% (v/v) DHP | | 23.5 | 17.6 | -156.6 | 68.8 |
| 40% (v/v) DHP | | 21.0 | 14.3 | -166.9 | 69.4 |
| 50% (v/v) DHP | | 24.4 | 20.0 | -157.9 | 70.1 |
| 60% (v/v) DHP | | 5.2 | 14.9 | -225.7 | 71.6 |
| Blank, 0% (v/v) DHP | 300 | 32.0 | 29.4 | -116.3 | 65.0 |
| 10% (v/v) DHP | | 20.7 | 16.1 | -159.5 | 66.9 |
| 20% (v/v) DHP | | 16.9 | 20.0 | -174.2 | 67.6 |
| 30% (v/v) DHP | | 21.9 | 18.1 | -160.1 | 68.3 |
| 40% (v/v) DHP | | 19.8 | 15.5 | -169.1 | 69.0 |
| 50% (v/v) DHP | | 23.3 | 15.6 | -159.5 | 69.5 |
| 60% (v/v) DHP | | 18.1 | 12.6 | -180.9 | 70.8 |
| Blank, 0% (v/v) DHP | 400 | 29.0 | 26.5 | -124.9 | 64.6 |
| 10% (v/v) DHP | | 21.1 | 15.9 | -156.5 | 66.4 |
| 20% (v/v) DHP | | 15.7 | 22.3 | -176.6 | 67.1 |
| 30% (v/v) DHP | | 20.4 | 18.3 | -163.4 | 67.8 |
| 40% (v/v) DHP | | 14.2 | 14.5 | -185.8 | 68.4 |
| 50% (v/v) DHP | | 25.4 | 14.6 | -151.7 | 69.2 |
| 60% (v/v) DHP | | 14.4 | 19.3 | -191.5 | 70.4 |
| Blank, 0% (v/v) DHP | 500 | 26.7 | 24.2 | -131.5 | 64.3 |
| 10% (v/v) DHP | | 21.8 | 16.4 | -153.1 | 66.1 |
| 20% (v/v) DHP | | 16.7 | 21.9 | -172.0 | 66.7 |
| 30% (v/v) DHP | | 23.2 | 17.8 | -153.2 | 67.5 |
| 40% (v/v) DHP | | 19.4 | 18.6 | -167.9 | 68.2 |
| 50% (v/v) DHP | | 20.1 | 23.2 | -168.8 | 69.1 |
| 60% (v/v) DHP | | 19.0 | 18.4 | -175.1 | 70.0 |
| Blank, 0% (v/v) DHP | 600 | 30.1 | 27.6 | -119.0 | 63.9 |
| 10% (v/v) DHP | | 21.0 | 16.1 | -154.9 | 65.8 |
| 20% (v/v) DHP | | 15.9 | 19.1 | -173.9 | 66.4 |
| 30% (v/v) DHP | | 24.3 | 18.6 | -148.7 | 67.2 |
| 40% (v/v) DHP | | 21.4 | 18.4 | -160.7 | 68.0 |
| 50% (v/v) DHP | | 29.1 | 27.2 | -138.1 | 68.7 |
| 60% (v/v) DHP | | 30.5 | 21.6 | -136.4 | 69.6 |
| Blank, 0% (v/v) DHP | 700 | 33.5 | 30.9 | -107.1 | 63.7 |
| 10% (v/v) DHP | | 20.9 | 16.9 | -154.5 | 65.6 |
| 20% (v/v) DHP | | 19.0 | 24.9 | -162.9 | 66.2 |
| 30% (v/v) DHP | | 21.0 | 17.6 | -158.7 | 67.0 |
| 40% (v/v) DHP | | 20.2 | 16.2 | -163.9 | 67.7 |
| 50% (v/v) DHP | | 34.3 | 25.0 | -120.1 | 68.5 |
| 60% (v/v) DHP | | 32.8 | 26.7 | -127.8 | 69.3 |
| Blank, 0% (v/v) DHP | 800 | 29.8 | 27.3 | -118.4 | 63.5 |
| 10% (v/v) DHP | | 22.8 | 19.4 | -147.7 | 65.4 |
| 20% (v/v) DHP | | 19.8 | 22.4 | -159.4 | 66.0 |
| 30% (v/v) DHP | | 23.2 | 17.0 | -150.8 | 66.7 |
| 40% (v/v) DHP | | 25.7 | 17.9 | -145.1 | 67.4 |
| 50% (v/v) DHP | | 35.9 | 24.9 | -114.2 | 68.2 |
| 60% (v/v) DHP | | 29.0 | 24.2 | -139.9 | 69.2 |
| Blank, 0% (v/v) DHP | 900 | 30.2 | 27.7 | -116.6 | 63.3 |
| 10% (v/v) DHP | | 22.1 | 21.2 | -149.5 | 65.2 |
| 20% (v/v) DHP | | 25.7 | 28.7 | -139.6 | 65.8 |
| 30% (v/v) DHP | | 23.2 | 19.5 | -150.5 | 66.6 |
| 40% (v/v) DHP | | 25.0 | 21.5 | -146.5 | 67.2 |
| 50% (v/v) DHP | | 36.0 | 24.9 | -113.3 | 68.1 |
| 60% (v/v) DHP | | 35.9 | 25.4 | -116.4 | 68.9 |
| Blank, 0% (v/v) DHP | 1000 | 30.5 | 28.0 | -114.9 | 63.1 |
| 10% (v/v) DHP | | 22.7 | 17.6 | -146.7 | 65.0 |
| 20% (v/v) DHP | | 23.1 | 29.2 | -147.6 | 65.7 |
| 30% (v/v) DHP | | 22.6 | 17.6 | -151.8 | 66.4 |
| 40% (v/v) DHP | | 27.8 | 20.6 | -136.9 | 67.1 |
| 50% (v/v) DHP | | 37.6 | 22.2 | -107.3 | 67.9 |
| 60% (v/v) DHP | | 32.9 | 24.0 | -125.5 | 68.7 |

The activation energy of the process, $E_a$, is an important parameter for determining the rate-controlling step. If the rate-controlling step is the diffusion of aqueous species in the boundary layer, then $E_a$ is generally $\leq$ 28 k J $mol^{-1}$, while $E_a$ is usually > 43 k J $mol^{-1}$ if adsorption of species on the reaction surface and subsequent chemical reaction takes place.

Values of activation energy, $E_a$, as well as the rest of thermodynamic parameters, enthalpy of activation, $\Delta H^*$, entropy of activation, $\Delta S^*$, and free energy of activation, $\Delta G^*$, were calculated and listed in Table 6.

Table 6 shows that all $E_a$ values are lower than 43 k J $mol^{-1}$, characterizing diffusion processes are controlling the electrodeposition reaction. Fig. 3 is a presentation of controlling the particle size as a parameter of two variables: the composition of DHP and the speed of rotation. As it is shown in Fig. 3, the highest composition of DHP does not mean the lowest $E_a$ value and vice-versa. This last observation is also applicable for forced convection regime.

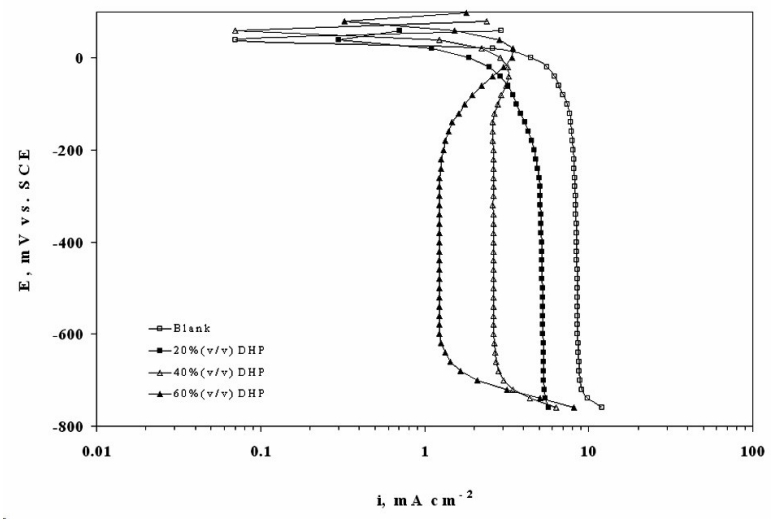


**Figure 3**. Variation of activation energy, $E_a$, (k J $mol^{-1}$) with the speed of rotation, rpm, at 298 K.

From Table 6, it is also noticed that the weak dependence of $\Delta G^*$ on the composition of the organic solvent can be attributable largely to the general linear compensation between $\Delta H^*$ and $\Delta S^*$ for the given temperature. The non linear variation of $\Delta S^*$ with the mole fraction is a criterion of specific solvation where random distribution is not valid in the absence of strong hydrogen bonding between the molecules of water and the organic solvent [18].

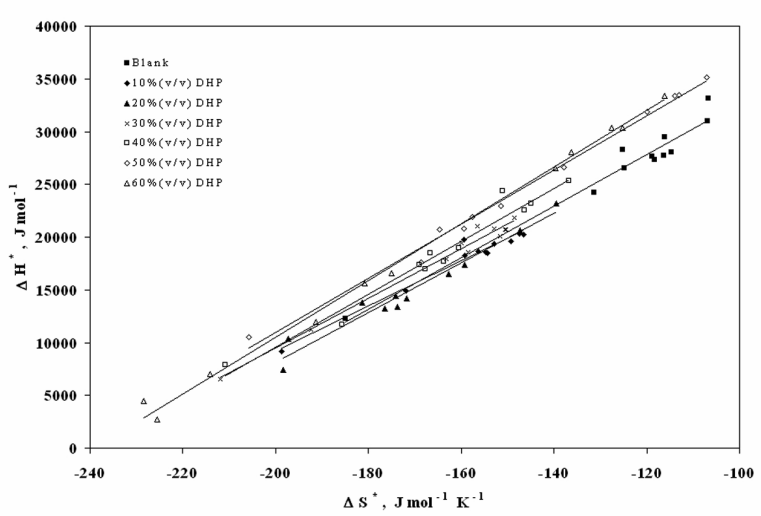


**Figure 4**.Variation of enthalpy of activation, $\Delta H^*$, (k J $mol^{-1}$) with the entropy of activation, $\Delta S^*$, (J $mole^{-1}$ $K^{-1}$).

The plots of $\Delta H^*$ versus $\Delta S^*$, Fig. 4, for different solvent compositions at different speeds of rotation were found to be linear. The values of isokinetic temperature, β, were computed from the slope of such plots and found to be in the range 214.3 – 269.0 K indicating that mass transfer rate is entropy controlled [19] where the solute-solvent interaction plays an important role in the rate determining step.

*Effect of rotation*

The angular velocity, ω, is given by equation 8:

$$\omega = \frac{2\pi \mathrm{rpm}}{60} \tag{8}$$

Fig. 5 shows the relation between the limiting current density and the angular velocity to a power 0.7 at 298 K and different compositions of DHP. Straight lines were obtained and the limiting current density increases by increasing rotation, which indicates that the electrodeposition process of copper in presence of DHP as well as in aqueous media is a diffusion-controlled reaction.

The diffusion coefficient of $Cu^{2+}$ ions, D, in different solutions was determined from the values of limiting current density, as shown in Table 7, using Eisenberg equation [3]:

$$i_l = 0.0791 n F C_b U^{0.7} d_i^{-0.3} \nu^{-0.344} D^{0.644} \tag{9}$$

where $C_b$ is the bulk concentration (mol $cm^{-3}$), U is the peripheral velocity = ωr in cm rad $s^{-1}$ (r is the radial distance in cm) or U = 2 πωr in cm $s^{-1}$, d is the characteristic length for the rotating cylinder in cm, and ν is the kinematic

viscosity in stoke ($\nu = \eta/\rho$, $\eta$ is the viscosity in g $cm^{-1}$ $s^{-1}$ and $\rho$ is the density in g $cm^{-3}$).

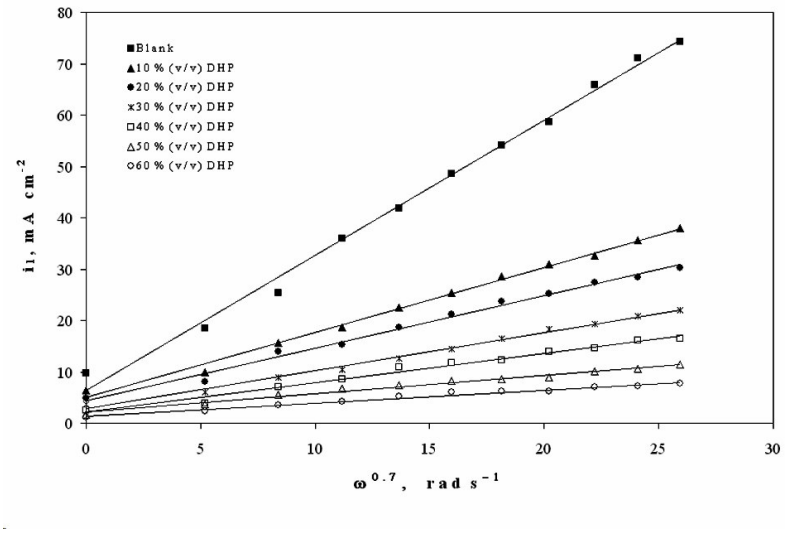


**Figure 5**. Variation of the limiting current density, $i_l$, with the angular velocity to a power 0.7, $\omega^{0.7}$, at 298 K, using different DHP contents.

The diffusion coefficient, D, of $Cu^{2+}$ ions in solutions containing alcohols decreases due to the increase in the interfacial viscosity [20], $\eta$, in accordance with the Stokes-Einstein equation:

$$\frac{\eta D}{T} = \text{const.} \qquad (10)$$

The present results agree with the polarographic studies [21,22] conducted in solutions containing surfactants where it was found that the diffusion current decreases in the presence of surfactants.

Table 7 illustrates the slight decrease in the values of the diffusion coefficient, D, in presence of DHP, which indicates that DHP hinders the diffusion of cupric ions from the bulk to the outer limit of the electrode double layer. A possible explanation is that DHP is a polar molecule with interfacial activity that could change the composition and the properties of the double layer on the electrode surface. Thus, DHP molecules replace the water molecules on the metallic surface, forming an adsorbed superficial film. This would increase the electrolyte viscosity and lower the dielectric constant at the electrode/electrolyte interface [23]. Consequently, hydrated metal ions or complex ions approach the surface with increased difficulty to enable charge transfer.

**Table 7**. Values of diffusion coefficient (D) for all mixtures at different temperatures.

| | rpm | 298 K | 303 K | 308 K | 313 K |
|---|---|---|---|---|---|
| | | D x10$^5$, cm$^2$ s$^{-1}$ | D x10$^5$, cm$^2$ s$^{-1}$ | D x10$^5$, cm$^2$ s$^{-1}$ | D x10$^5$, cm$^2$ s$^{-1}$ |
| Blank, 0% (v/v) DHP | 100 | 1.280 | 1.866 | 2.305 | 2.530 |
| | 200 | 1.016 | 1.439 | 1.441 | 2.468 |
| | 300 | 0.987 | 1.348 | 1.735 | 2.208 |
| | 400 | 0.918 | 1.268 | 1.497 | 1.914 |
| | 500 | 0.904 | 1.216 | 1.266 | 1.825 |
| | 600 | 0.879 | 1.291 | 1.463 | 1.928 |
| | 700 | 0.842 | 1.136 | 1.637 | 1.908 |
| | 800 | 0.873 | 1.179 | 1.450 | 1.848 |
| | 900 | 0.864 | 1.134 | 1.550 | 1.785 |
| | 1000 | 0.825 | 1.167 | 1.413 | 1.796 |
| 10% (v/v) DHP | 100 | 0.451 | 0.568 | 0.626 | 0.769 |
| | 200 | 0.432 | 0.510 | 0.537 | 0.636 |
| | 300 | 0.365 | 0.443 | 0.511 | 0.582 |
| | 400 | 0.358 | 0.446 | 0.486 | 0.590 |
| | 500 | 0.336 | 0.433 | 0.487 | 0.561 |
| | 600 | 0.332 | 0.405 | 0.457 | 0.539 |
| | 700 | 0.317 | 0.395 | 0.453 | 0.509 |
| | 800 | 0.298 | 0.396 | 0.443 | 0.514 |
| | 900 | 0.302 | 0.383 | 0.437 | 0.505 |
| | 1000 | 0.297 | 0.378 | 0.424 | 0.512 |
| 20% (v/v) DHP | 100 | 0.355 | 0.386 | 0.449 | 0.488 |
| | 200 | 0.387 | 0.386 | 0.415 | 0.440 |
| | 300 | 0.288 | 0.305 | 0.349 | 0.406 |
| | 400 | 0.288 | 0.284 | 0.333 | 0.387 |
| | 500 | 0.274 | 0.321 | 0.348 | 0.390 |
| | 600 | 0.268 | 0.295 | 0.330 | 0.368 |
| | 700 | 0.249 | 0.301 | 0.323 | 0.384 |
| | 800 | 0.245 | 0.273 | 0.310 | 0.382 |
| | 900 | 0.228 | 0.272 | 0.315 | 0.430 |
| | 1000 | 0.225 | 0.260 | 0.304 | 0.388 |
| 30% (v/v) DHP | 100 | 0.249 | 0.244 | 0.243 | 0.332 |
| | 200 | 0.208 | 0.232 | 0.309 | 0.347 |
| | 300 | 0.173 | 0.247 | 0.240 | 0.303 |
| | 400 | 0.171 | 0.241 | 0.243 | 0.282 |
| | 500 | 0.163 | 0.206 | 0.236 | 0.284 |
| | 600 | 0.166 | 0.197 | 0.234 | 0.295 |
| | 700 | 0.165 | 0.193 | 0.224 | 0.265 |
| | 800 | 0.155 | 0.197 | 0.224 | 0.270 |
| | 900 | 0.152 | 0.183 | 0.213 | 0.263 |
| | 1000 | 0.149 | 0.186 | 0.209 | 0.256 |
| 40% (v/v) DHP | 100 | 0.136 | 0.236 | 0.252 | 0.272 |
| | 200 | 0.164 | 0.173 | 0.218 | 0.256 |
| | 300 | 0.142 | 0.153 | 0.180 | 0.219 |
| | 400 | 0.150 | 0.170 | 0.175 | 0.200 |
| | 500 | 0.132 | 0.142 | 0.163 | 0.202 |
| | 600 | 0.116 | 0.139 | 0.157 | 0.190 |
| | 700 | 0.119 | 0.137 | 0.151 | 0.189 |
| | 800 | 0.111 | 0.133 | 0.168 | 0.202 |
| | 900 | 0.113 | 0.130 | 0.173 | 0.199 |
| | 1000 | 0.104 | 0.121 | 0.165 | 0.200 |
| 50% (v/v) DHP | 100 | 0.140 | 0.160 | 0.196 | 0.237 |
| | 200 | 0.121 | 0.116 | 0.178 | 0.200 |
| | 300 | 0.108 | 0.125 | 0.168 | 0.178 |
| | 400 | 0.090 | 0.099 | 0.141 | 0.157 |
| | 500 | 0.084 | 0.088 | 0.111 | 0.128 |
| | 600 | 0.074 | 0.086 | 0.116 | 0.149 |
| | 700 | 0.066 | 0.084 | 0.115 | 0.158 |
| | 800 | 0.070 | 0.082 | 0.119 | 0.172 |
| | 900 | 0.065 | 0.083 | 0.117 | 0.163 |
| | 1000 | 0.066 | 0.081 | 0.105 | 0.178 |
| 60% (v/v) DHP | 100 | 0.158 | 0.085 | 0.091 | 0.088 |
| | 200 | 0.137 | 0.069 | 0.068 | 0.067 |
| | 300 | 0.122 | 0.059 | 0.081 | 0.082 |
| | 400 | 0.102 | 0.060 | 0.071 | 0.078 |
| | 500 | 0.095 | 0.058 | 0.066 | 0.089 |
| | 600 | 0.084 | 0.053 | 0.069 | 0.108 |
| | 700 | 0.075 | 0.065 | 0.083 | 0.099 |
| | 800 | 0.079 | 0.057 | 0.076 | 0.092 |
| | 900 | 0.074 | 0.060 | 0.088 | 0.100 |
| | 1000 | 0.074 | 0.071 | 0.087 | 0.096 |

It was noted in a previous review [24] that mass transport to an inner RCE in turbulent flow system may be described by empirical dimensionless correlations of the form:

$$Sh = a\,Re^{b}\,.Sc^{c} \qquad (11)$$

where Sh, Re and Sc are the Sherwood (Sh=kl/D), Reynolds (Re=lU/ν) and Schmidt (Sc=ν/D) numbers, respectively, and a and b are empirical constants, c = 0.33, indicating forced convection regime [1]. Table 8 summarizes the values of dimensionless groups (Sh, Sc and Re) at all experimental conditions. By plotting $\log\left[\frac{Sh}{Sc^{0.33}}\right]$ against $\log(Re)$, a straight line was obtained which slope gave the constant b while the intercept offered the other constant a, Table 9. Values of constants a and b depend on [24]: i) the type of roughness, ii) the degree of roughness, and iii) the electrolyte composition, temperature and the morphology of the deposits.

In this study, a forced convection mechanism is obtained which agrees very well with the relationship $Sh = 0.0791\,Re^{0.7}\,Sc^{0.356}$ given by Eisenberg et al. [25] for mass transfer to a rotating cylinder in turbulent flow system and exponents in all equations denote a highly turbulent flow, which agrees with the previous mass transfer study in aqueous media [26]. Also, results at hand agree excellently with $Sh = 1.581\,Re^{0.725}\,Sc^{0.33}$ given by Mamdouh et al. [27] for mass transfer during cementation using rotating cylinder in an aqueous medium as well as with the equation $Sh = 0.061\,Re^{0.833}\,Sc^{0.33}$ given by Ahmed et al. [28] for mass transfer during copper cementation from alcoholic-water mixtures using rotating cylinder in turbulent system.

*Determination of the critical velocity*

To evaluate whether the limiting current increases indefinitely with increasing the speed of rotation or there is a limit for such increase, two solutions were chosen: one of them was the blank solution and the other was 20% (v/v) DHP. Polarisations were carried out at high speeds of rotation and 298 K. Fig. 6 shows the relation between the limiting current density and the angular velocity, ω, to a power 0.7 for blank and 20% (v/v) DHP solutions at 298 K and high speeds of rotation. It is shown in Table 10 that the critical velocity in case of blank solution in the range of 5000 – 6000 rpm with average critical limiting current density of 148.91 mA $cm^{-2}$, while for 20% (v/v) DHP solution it was 5500 – 7000 rpm with average limiting current density of 101.34 mA $cm^{-2}$. Currently, it is clear that the presence of DHP in the medium increases the critical velocity and decreases the critical limiting current density. This leads to conclude that the presence of DHP in copper electrodeposition bath will offer a faster surface diffusion process compared with electron transfer and as a result the formation of adatoms and both crystal lattices and surface features will be well formed [29].

**Table 8a**. Dimensionless groups used in dimensional analysis for all solutions at 298 and 303 K.

| | rpm | 298 K | | | 303 K | | |
|---|---|---|---|---|---|---|---|
| | | *Sh=kl/D* | *Sc=ν/D* | *Re=lU/ν* | *Sh=kl/D* | *Sc=ν/D* | *Re=lU/ν* |
| Blank, 0% (v/v) DHP | 100 | 92 | 771 | 705 | 83 | 475 | 784 |
| | 200 | 162 | 971 | 1409 | 148 | 616 | 1568 |
| | 300 | 217 | 1000 | 2114 | 202 | 658 | 2351 |
| | 400 | 272 | 1075 | 2818 | 252 | 699 | 3135 |
| | 500 | 320 | 1091 | 3523 | 299 | 729 | 3919 |
| | 600 | 368 | 1122 | 4228 | 332 | 687 | 4703 |
| | 700 | 416 | 1172 | 4932 | 388 | 780 | 5486 |
| | 800 | 451 | 1129 | 5637 | 420 | 752 | 6270 |
| | 900 | 491 | 1142 | 6342 | 462 | 782 | 7054 |
| | 1000 | 538 | 1196 | 7046 | 493 | 760 | 7838 |
| 10% (v/v) DHP | 100 | 131 | 2262 | 681 | 126 | 1614 | 757 |
| | 200 | 217 | 2364 | 1362 | 212 | 1798 | 1514 |
| | 300 | 306 | 2797 | 2042 | 296 | 2070 | 2272 |
| | 400 | 377 | 2853 | 2723 | 361 | 2059 | 3029 |
| | 500 | 450 | 3037 | 3404 | 426 | 2117 | 3786 |
| | 600 | 514 | 3077 | 4085 | 496 | 2265 | 4543 |
| | 700 | 582 | 3225 | 4765 | 558 | 2326 | 5301 |
| | 800 | 653 | 3429 | 5446 | 612 | 2320 | 6058 |
| | 900 | 706 | 3383 | 6127 | 672 | 2395 | 6815 |
| | 1000 | 764 | 3437 | 6808 | 728 | 2429 | 7572 |
| 20% (v/v) DHP | 100 | 137 | 3291 | 594 | 137 | 2722 | 661 |
| | 200 | 215 | 3023 | 1189 | 223 | 2723 | 1322 |
| | 300 | 317 | 4060 | 1783 | 323 | 3446 | 1983 |
| | 400 | 388 | 4062 | 2377 | 405 | 3700 | 2644 |
| | 500 | 462 | 4270 | 2971 | 453 | 3278 | 3305 |
| | 600 | 529 | 4357 | 3566 | 531 | 3569 | 3966 |
| | 700 | 605 | 4703 | 4160 | 586 | 3490 | 4627 |
| | 800 | 668 | 4782 | 4754 | 666 | 3844 | 5288 |
| | 900 | 744 | 5121 | 5348 | 725 | 3859 | 5949 |
| | 1000 | 805 | 5202 | 5943 | 793 | 4045 | 6610 |
| 30% (v/v) DHP | 100 | 147 | 5483 | 508 | 153 | 5040 | 565 |
| | 200 | 254 | 6583 | 1016 | 254 | 5306 | 1130 |
| | 300 | 361 | 7922 | 1524 | 329 | 4974 | 1695 |
| | 400 | 443 | 8009 | 2032 | 407 | 5111 | 2260 |
| | 500 | 526 | 8375 | 2540 | 503 | 5979 | 2825 |
| | 600 | 595 | 8264 | 3048 | 581 | 6256 | 3391 |
| | 700 | 664 | 8302 | 3556 | 651 | 6372 | 3956 |
| | 800 | 745 | 8815 | 4064 | 710 | 6254 | 4521 |
| | 900 | 814 | 8981 | 4572 | 792 | 6735 | 5086 |
| | 1000 | 883 | 9159 | 5080 | 847 | 6623 | 5651 |
| 40% (v/v) DHP | 100 | 170 | 12139 | 420 | 145 | 6302 | 467 |
| | 200 | 259 | 10099 | 840 | 264 | 8605 | 935 |
| | 300 | 362 | 11645 | 1261 | 366 | 9701 | 1402 |
| | 400 | 434 | 11008 | 1681 | 432 | 8763 | 1870 |
| | 500 | 532 | 12563 | 2101 | 537 | 10463 | 2337 |
| | 600 | 633 | 14308 | 2521 | 615 | 10690 | 2804 |
| | 700 | 699 | 13912 | 2941 | 689 | 10861 | 3272 |
| | 800 | 786 | 14903 | 3362 | 765 | 11217 | 3739 |
| | 900 | 847 | 14593 | 3782 | 836 | 11407 | 4207 |
| | 1000 | 939 | 15826 | 4202 | 923 | 12240 | 4674 |
| 50% (v/v) DHP | 100 | 157 | 14565 | 342 | 156 | 11415 | 380 |
| | 200 | 269 | 16733 | 684 | 283 | 15767 | 761 |
| | 300 | 372 | 18837 | 1026 | 366 | 14614 | 1141 |
| | 400 | 486 | 22573 | 1368 | 488 | 18513 | 1521 |
| | 500 | 581 | 24140 | 1710 | 593 | 20729 | 1902 |
| | 600 | 691 | 27402 | 2052 | 679 | 21195 | 2282 |
| | 700 | 801 | 30637 | 2394 | 764 | 21723 | 2662 |
| | 800 | 862 | 28991 | 2736 | 845 | 22242 | 3043 |
| | 900 | 960 | 31091 | 3078 | 915 | 22006 | 3423 |
| | 1000 | 1032 | 30937 | 3419 | 994 | 22612 | 3804 |
| 60% (v/v) DHP | 100 | 139 | 16218 | 271 | 180 | 27130 | 302 |
| | 200 | 238 | 18633 | 543 | 314 | 33190 | 604 |
| | 300 | 329 | 20976 | 814 | 443 | 39275 | 906 |
| | 400 | 429 | 25135 | 1086 | 536 | 38119 | 1208 |
| | 500 | 514 | 26880 | 1357 | 637 | 39764 | 1510 |
| | 600 | 611 | 30512 | 1629 | 747 | 43491 | 1812 |
| | 700 | 708 | 34115 | 1900 | 774 | 35566 | 2114 |
| | 800 | 762 | 32281 | 2172 | 887 | 40101 | 2416 |
| | 900 | 849 | 34620 | 2443 | 947 | 38227 | 2718 |
| | 1000 | 912 | 34448 | 2715 | 964 | 32599 | 3020 |

**Table 8b**. Dimensionless groups used in dimensional analysis for all solutions at 308 and 313 K.

| % (v/v) DHP | rpm | 308 K | | | 313 K | | |
|---|---|---|---|---|---|---|---|
| | | *Sh=kl/D* | *Sc=ν/D* | *Re=lU/ν* | *Sh=kl/D* | *Sc=ν/D* | *Re=lU/ν* |
| Blank, 0% (v/v) DHP | 100 | 80 | 349 | 865 | 80 | 290 | 948 |
| | 200 | 153 | 557 | 1730 | 131 | 297 | 1896 |
| | 300 | 191 | 463 | 2595 | 180 | 332 | 2844 |
| | 400 | 246 | 536 | 3460 | 232 | 383 | 3792 |
| | 500 | 305 | 634 | 4325 | 276 | 402 | 4740 |
| | 600 | 329 | 549 | 5190 | 308 | 380 | 5688 |
| | 700 | 352 | 491 | 6055 | 344 | 384 | 6636 |
| | 800 | 404 | 554 | 6920 | 382 | 397 | 7584 |
| | 900 | 428 | 518 | 7785 | 420 | 411 | 8533 |
| | 1000 | 476 | 568 | 8650 | 451 | 408 | 9481 |
| 10% (v/v) DHP | 100 | 125 | 1328 | 836 | 120 | 987 | 916 |
| | 200 | 215 | 1549 | 1671 | 209 | 1193 | 1832 |
| | 300 | 291 | 1628 | 2507 | 287 | 1303 | 2748 |
| | 400 | 362 | 1709 | 3343 | 349 | 1287 | 3664 |
| | 500 | 423 | 1709 | 4179 | 415 | 1351 | 4580 |
| | 600 | 492 | 1818 | 5014 | 479 | 1407 | 5496 |
| | 700 | 550 | 1836 | 5850 | 544 | 1489 | 6412 |
| | 800 | 608 | 1876 | 6686 | 596 | 1477 | 7328 |
| | 900 | 664 | 1905 | 7522 | 651 | 1501 | 8244 |
| | 1000 | 722 | 1960 | 8357 | 697 | 1483 | 9160 |
| 20% (v/v) DHP | 100 | 135 | 2124 | 730 | 135 | 1782 | 800 |
| | 200 | 225 | 2297 | 1459 | 228 | 1974 | 1599 |
| | 300 | 318 | 2731 | 2189 | 311 | 2139 | 2399 |
| | 400 | 396 | 2861 | 2918 | 387 | 2243 | 3198 |
| | 500 | 455 | 2736 | 3648 | 451 | 2231 | 3998 |
| | 600 | 527 | 2889 | 4377 | 523 | 2361 | 4798 |
| | 700 | 592 | 2952 | 5107 | 574 | 2266 | 5597 |
| | 800 | 659 | 3068 | 5836 | 632 | 2278 | 6397 |
| | 900 | 712 | 3022 | 6566 | 658 | 2021 | 7196 |
| | 1000 | 776 | 3138 | 7296 | 734 | 2241 | 7996 |
| 30% (v/v) DHP | 100 | 159 | 4577 | 624 | 147 | 3060 | 684 |
| | 200 | 237 | 3607 | 1247 | 235 | 2933 | 1367 |
| | 300 | 344 | 4642 | 1871 | 327 | 3353 | 2051 |
| | 400 | 420 | 4593 | 2495 | 411 | 3608 | 2734 |
| | 500 | 496 | 4728 | 3118 | 479 | 3578 | 3418 |
| | 600 | 564 | 4755 | 3742 | 537 | 3450 | 4101 |
| | 700 | 639 | 4983 | 4366 | 621 | 3832 | 4785 |
| | 800 | 702 | 4984 | 4989 | 677 | 3759 | 5468 |
| | 900 | 775 | 5232 | 5613 | 742 | 3867 | 6152 |
| | 1000 | 840 | 5332 | 6237 | 807 | 3973 | 6836 |
| 40% (v/v) DHP | 100 | 147 | 5346 | 516 | 148 | 4515 | 565 |
| | 200 | 251 | 6177 | 1032 | 245 | 4796 | 1131 |
| | 300 | 357 | 7466 | 1548 | 344 | 5615 | 1696 |
| | 400 | 442 | 7710 | 2063 | 434 | 6133 | 2262 |
| | 500 | 530 | 8280 | 2579 | 506 | 6081 | 2827 |
| | 600 | 609 | 8565 | 3095 | 588 | 6466 | 3392 |
| | 700 | 688 | 8892 | 3611 | 656 | 6497 | 3958 |
| | 800 | 727 | 8007 | 4127 | 703 | 6074 | 4523 |
| | 900 | 782 | 7783 | 4643 | 768 | 6170 | 5088 |
| | 1000 | 857 | 8172 | 5159 | 825 | 6133 | 5654 |
| 50% (v/v) DHP | 100 | 150 | 8465 | 420 | 144 | 6364 | 460 |
| | 200 | 252 | 9295 | 840 | 249 | 7568 | 920 |
| | 300 | 341 | 9858 | 1259 | 345 | 8486 | 1380 |
| | 400 | 444 | 11723 | 1679 | 442 | 9645 | 1840 |
| | 500 | 565 | 14860 | 2099 | 555 | 11831 | 2300 |
| | 600 | 633 | 14304 | 2519 | 597 | 10133 | 2761 |
| | 700 | 706 | 14348 | 2939 | 652 | 9580 | 3221 |
| | 800 | 767 | 13931 | 3358 | 693 | 8756 | 3681 |
| | 900 | 837 | 14139 | 3778 | 769 | 9293 | 4141 |
| | 1000 | 938 | 15800 | 4198 | 801 | 8486 | 4601 |
| 60% (v/v) DHP | 100 | 181 | 22797 | 333 | 190 | 21614 | 365 |
| | 200 | 328 | 30803 | 667 | 339 | 28244 | 731 |
| | 300 | 409 | 25872 | 1000 | 420 | 23213 | 1096 |
| | 400 | 523 | 29266 | 1333 | 522 | 24242 | 1461 |
| | 500 | 630 | 31754 | 1666 | 584 | 21484 | 1826 |
| | 600 | 701 | 30046 | 2000 | 618 | 17609 | 2192 |
| | 700 | 734 | 25221 | 2333 | 711 | 19250 | 2557 |
| | 800 | 832 | 27562 | 2666 | 800 | 20655 | 2922 |
| | 900 | 856 | 23683 | 2999 | 845 | 19060 | 3287 |
| | 1000 | 927 | 24087 | 3333 | 922 | 19793 | 3653 |

**Table 9**. Dimensionless correlation constants a and b under all study conditions.

| | 298 K | 303 K | 308 K | 313 K |
|---|---|---|---|---|
| **Constant *a*** | | | | |
| Blank, 0% (v/v) DHP | 0.1010 | 0.0993 | 0.0996 | 0.0982 |
| 10% (v/v) DHP | 0.1031 | 0.1026 | 0.1025 | 0.1014 |
| 20% (v/v) DHP | 0.1036 | 0.1042 | 0.1036 | 0.1046 |
| 30% (v/v) DHP | 0.1058 | 0.1063 | 0.1065 | 0.1052 |
| 40% (v/v) DHP | 0.1084 | 0.1055 | 0.1060 | 0.1060 |
| 50% (v/v) DHP | 0.1058 | 0.1064 | 0.1055 | 0.1074 |
| 60% (v/v) DHP | 0.1063 | 0.1124 | 0.1138 | 0.1157 |
| **Constant *b*** | | | | |
| Blank, 0% (v/v) DHP | 0.7044 | 0.7051 | 0.7038 | 0.7044 |
| 10% (v/v) DHP | 0.7052 | 0.7046 | 0.7041 | 0.7046 |
| 20% (v/v) DHP | 0.7059 | 0.7044 | 0.7044 | 0.7023 |
| 30% (v/v) DHP | 0.7054 | 0.7037 | 0.7027 | 0.7033 |
| 40% (v/v) DHP | 0.7040 | 0.7066 | 0.7049 | 0.7040 |
| 50% (v/v) DHP | 0.7096 | 0.7078 | 0.7074 | 0.7039 |
| 60% (v/v) DHP | 0.7096 | 0.7029 | 0.7000 | 0.6970 |

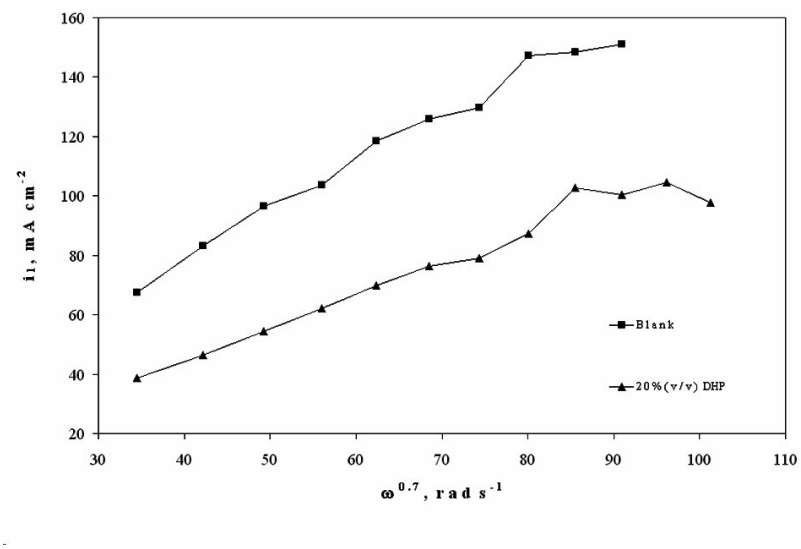


**Figure 6**. Variation of the limiting current density, $i_l$, with the angular velocity to a power 0.7, $\omega^{0.7}$, at high speeds of rotation and 298 K.

It can be noticed from Fig. 6 that the limiting current density increases by increasing rotation until we reach a certain region at which the current keeps almost constant: this is again the region of the critical velocity. Then the data at high speeds of rotation can be correlated by the equation, $Sh = 0.1022\,Re^{0.705}\,Sc^{0.33}$ as previously shown.

**Table 10**. Values of the limiting current density ($i_l$), angular velocity ($\omega$), kinematic viscosity ($\nu$), diffusion coefficient (D), and dimensionless groups used in dimensional analysis for blank and 20% (v/v) DHP at high speeds of rotation and 298 K.

| | $(i_l)$ mA cm$^{-2}$ | rpm | $\omega$ | $(\nu)$, stoke | (D) x 10$^5$, cm$^2$ s$^{-1}$ | $Sh=kl/D$ | $Sc=\nu/D$ | $Re=lU/\nu$ |
|---|---|---|---|---|---|---|---|---|
| Blank, 0% (v/v) DHP | 67.57 | 1500 | 157.1 | 0.0098616 | 0.458 | 912 | 2086 | 11294 |
| | 83.32 | 2000 | 209.4 | | 0.464 | 1110 | 2060 | 15059 |
| | 96.50 | 2500 | 261.8 | | 0.457 | 1305 | 2090 | 18823 |
| | 103.55 | 3000 | 314.2 | | 0.419 | 1530 | 2284 | 22588 |
| | 118.50 | 3500 | 366.5 | | 0.436 | 1679 | 2191 | 26352 |
| | 125.85 | 4000 | 418.9 | | 0.415 | 1877 | 2307 | 30117 |
| | 129.87 | 4500 | 471.2 | | 0.383 | 2097 | 2497 | 33882 |
| | 147.25 | 5000 | 523.6 | | 0.415 | 2194 | 2304 | 37646 |
| | 148.46 | 5500 | 576.0 | | 0.379 | 2422 | 2523 | 41411 |
| | 151.03 | 6000 | 628.3 | | 0.354 | 2638 | 2700 | 45176 |
| 20% (v/v) DHP | 38.62 | 1500 | 157.1 | 0.012545 | 0.186 | 1242 | 4973 | 11294 |
| | 46.51 | 2000 | 209.4 | | 0.181 | 1532 | 5094 | 15059 |
| | 54.30 | 2500 | 261.8 | | 0.181 | 1793 | 5105 | 18823 |
| | 62.02 | 3000 | 314.2 | | 0.182 | 2031 | 5062 | 22588 |
| | 69.81 | 3500 | 366.5 | | 0.185 | 2249 | 4981 | 26352 |
| | 76.33 | 4000 | 418.9 | | 0.184 | 2475 | 5014 | 30117 |
| | 78.91 | 4500 | 471.2 | | 0.171 | 2762 | 5412 | 33882 |
| | 87.20 | 5000 | 523.6 | | 0.178 | 2931 | 5197 | 37646 |
| | 102.85 | 5500 | 576.0 | | 0.207 | 2967 | 4461 | 41411 |
| | 100.31 | 6000 | 628.3 | | 0.181 | 3307 | 5098 | 45176 |
| | 104.62 | 6500 | 680.7 | | 0.177 | 3525 | 5209 | 48940 |
| | 97.60 | 7000 | 733.0 | | 0.147 | 3970 | 6289 | 52705 |

From the previous study concerning the electrodeposition process of copper powder in acidified solutions of copper sulphate and in the presence of DHP using the rotating cylinder electrode (RCE) the data were valid for $80 < Sh < 3970$, $290 < Sc < 59284$ and $271 < Re < 52705$.

*Morphology and composition analyses*

Since the concern was mainly the production of copper powder, all experiments were carried out at the limiting current that was determined for each solution, so it is expected that the morphologies of electrodeposited copper powder must be characterised by 3-D nucleation [7]. The phenomenon of dendritic growth [29] may occur if the rate of the electrodeposition process is partially diffusion controlled; so, on a microrough surface, the rate of deposition at surface peaks will be greater than that at troughs. These surface non-uniformities, therefore, become more pronounced resulting, eventually, in the formation of macrorough deposits. The phenomenon of dendritic growth may also be related to differences in the rate of diffusion at different points on a surface. In the case of macrospiral growth, for instance, spherical diffusion to the tip of the spiral results in a higher rate of mass transport to this point and this may lead to dendritic growth.

All experiments proceeded at 298 K with duration time of 20 minutes using copper anode and copper was electrodeposited onto copper cylinder with variation in the speed of rotation between 200 and 1000 rpm. Although it was stated [30] that an increase in copper ion concentration or in agitation will increase the particles size and obscures their dendritic character, it was found dramatic changes occurred when rotation started, dendrite nodules were formed

with high degree of discontinuity as well as very rough deposits as in case of blank solution at 200 rpm, Fig. 7a.

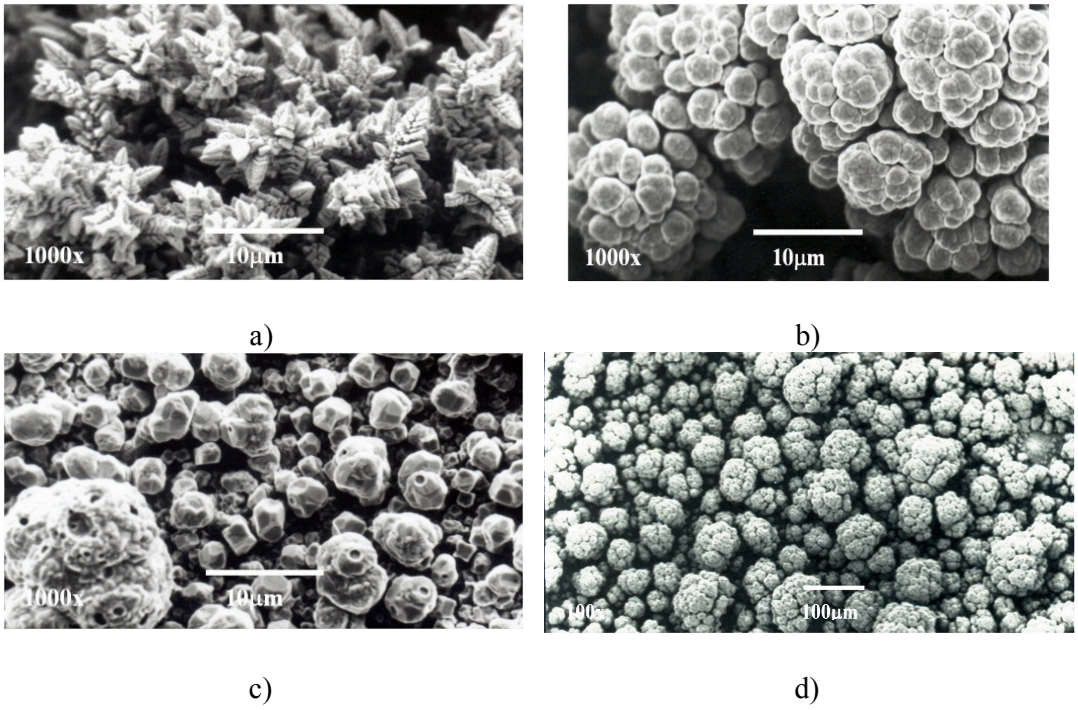


**Figure 7**. Electrodeposited copper in case of blank solution after 20 minutes a) at 25 – 26 mA $cm^{-2}$, 298 K and 200 rpm, b) at 74 – 75 mA $cm^{-2}$, 298 K and 1000 rpm, c) at 30 – 31 mA $cm^{-2}$, 298 K and 1000 rpm, and d) at 54 – 55 mA $cm^{-2}$, 298 K and 600 rpm.

Contrary to Fig. 7a at 200 rpm, grape-like aggregates were formed with low degree of discontinuity at 1000 rpm in case of blank solution, as shown in Fig. 7b. Fig. 7c represents the third type of morphology in this study in case of 20% (v/v) DHP at 1000 rpm, which is rounded-crystalline aggregates with voids. The main reason for voids formation is attributable to the swelling effect that correlates with the liberation of gases [31]. This structure is considered as a unique surface feature in this study, although case of 10% (v/v) DHP tends to give similar structure.

At 600 rpm for all solutions, except 20% (v/v) DHP, a transient structure between dendrite nodules and grape-like aggregates was formed, which means that the region between 200 – 600 rpm is considered as a transient region with mixed deposition mechanisms as shown in Fig. 7d in case of blank solution.

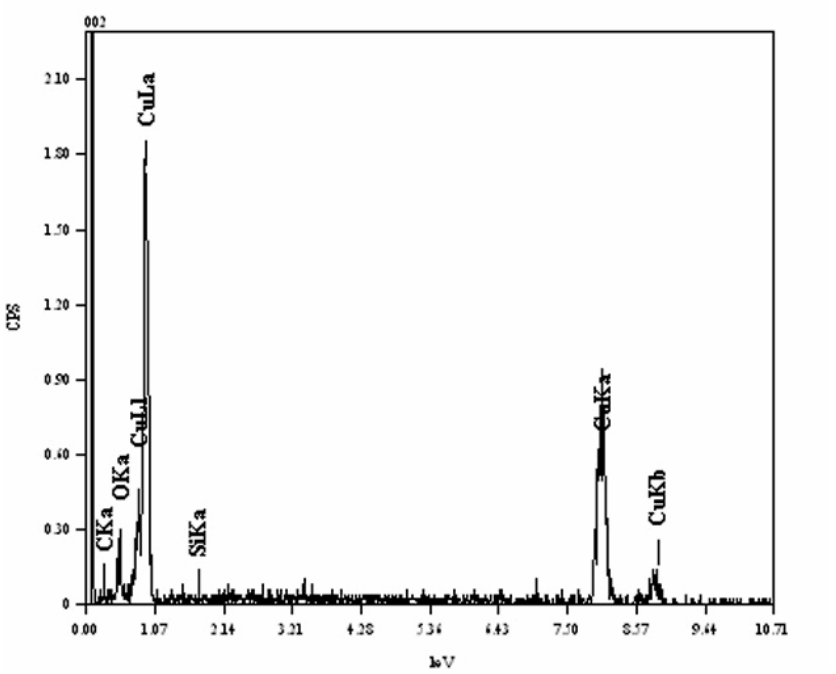


**Figure 8**. Deposit EDS analysis at different experimental conditions.

High current densities or high cathodic overpotentials, accompanied by fast stirring rates can adversely affect electrodeposition process resulting in brittle deposits, which can comprise occlusions of additives and/or foreign materials [32]. Fig. 8 gives the EDS analysis for some chosen specimens that represent most of the experimental conditions. The analysis indicated that the composition of the electrodeposited copper powder under different conditions for all solutions was mainly pure copper (80.24 at.%) and oxygen (19.37 at.%) with tiny percentage of silicon and carbon, which may be due to the occlusion of foreign materials [32] on one hand. On the other hand, the presence of silicon could be attributable to the attendance of some glass leftover from another specimen, while carbon is referable to the coating of specimen with carbon before the analysis. In addition, oxygen peak in Fig. 8 might be caused by the oxidation of a negligible part of the deposit due to the high voltage used in the analysis. Fig. 9 represents the distribution of both copper and oxygen in the produced powder under different conditions, showing the mutual homogeneous distribution of copper and oxygen.

XRD patterns of the deposited copper powder are presented in Fig. 10 as an example. This exhibits polycrystalline copper in as deposited state with (111) as prominent plane parallel to the substrate. According to the standard PDF card (No. 04-0836) [33] all of the detected peaks are indexed as those from the cubic crystal [space group Fm3m (225)] with small two peaks that patterned for $Cu_2O$. The average particle size was calculated using Scherrer's equation:

$$D = \frac{0.9\lambda}{B\cos\theta_B} \qquad (12)$$

where D is the particle size in nm, λ is the wave length of X-ray radiation source (Cu Ka1, λ = 1.54056), B is the full-width at half maximum and θ is the angle.

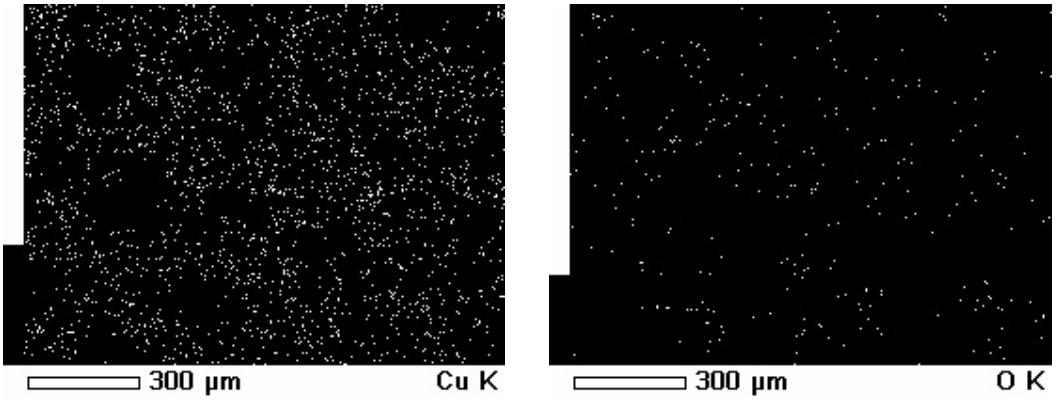


**a** **b**

**Figure 9**. Atomic distribution of **a**) Cu K and **b**) O K.

The average particle size of copper powder electrodeposited in absence of DHP was ranged between 127 nm at 1000 rpm and 132.8 nm at 0 rpm, except at 600 rpm which was 83.8 nm, supporting the hypothesis of transient mechanism at that rotation speed. Contrary to the blank solution, the average particle size in presence of DHP was 60.5 nm at all rotation speeds and all concentrations, except at 1000 rpm and 20% (v/v) DHP which was 203.4 nm, proving the unique structure of the deposited copper powder at that concentration.

## Conclusion

From the previous study concerning the electrodeposition process of copper powder in acidified solutions of copper sulphate and in the presence of DHP using the rotating cylinder electrode (RCE) the data were valid for $80 < Sh < 3970$, $290 < Sc < 59284$ and $271 < Re < 52705$ with overall dimensionless correlation of $Sh = 0.1022\,Re^{0.705}\,Sc^{0.33}$. Addition of DHP to the sulphate electrodeposition bath increases the cathodic polarisation and decreases the value of the limiting current density, while it increases with increasing temperature and the speed of rotation. The percentage of inhibition, P, was in the range 0.00 - 92.91% depending on the concentration of DHP as well as on the temperature. The adsorption of DHP on copper surface was found to be physical adsorption and obeyed both Langmuir and Temkin adsorption isotherms. The mass transfer rate was found to be entropy controlled with diffusion process controlling the electrodeposition. The range of the critical velocity in case of blank solution was 5000 – 6000 rpm with average critical limiting current density of 148.91 mA $cm^{-2}$, while it was 5500 – 7000 rpm for 20% (v/v) DHP solution with average limiting current density of 101.34 mA $cm^{-2}$.

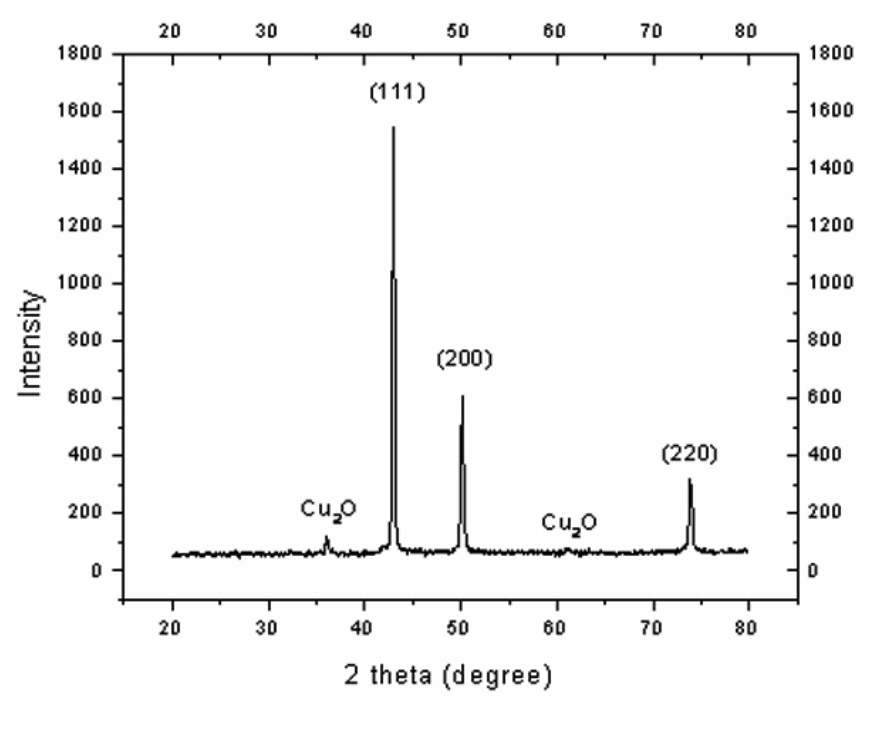


**Figure 10**. XRD patterns of deposited Cu powder at different experimental conditions.

3-D dendritic structures were formed when the electrodeposition was carried out at the limiting current density with various particle sizes ranged 60.5 – 203.4 nm. EDS elemental analysis and XRD diffraction patterns indicated that the formed powder was mainly copper (80.24 at.%) and oxygen (19.37 at.%) with traces of carbon (0.35 at.%) and silicon (0.04 at.%). The morphological structure of deposited copper from 20% (v/v) DHP at 1000 rpm and 298K was unique, rounded-crystalline aggregates with voids.

## References

1. D.R. Gabe, F.C. Walsh, *J. Appl. Electrochem.* 13 (1983) 3.
2. D.R. Gabe, F.C.Walsh, *The Reinhardt Schuhmann International Symposium on Innovative Technology and Reactor Design in Extraction Metallurgy*, Colorado Springs, Colorado, USA, 9-12 Nov. 1986, 775.
3. M. Eisenberg, C.W. Tobias, C.R. Wilke, *J. Electrochem. Soc.* 101 (1954) 306.
4. R. Winand, "*Application of Polarisation Measurements in the Control of Metal Deposition*", I.H. Warren, Elsevier Science Publishers, Amsterdam 1984, 47.
5. L. Muresan, S. Varvara, G. Maurin, S. Dorneanu, *Hydrometallurgy* 54(2-3) (2000) 161.
6. J.J. Kelly, C.Y. Tian, A.C. West, *J. Electrochem. Soc.* 146 (1999) 2540.

7. T.N. Andersen, C.H. Pitt, L.S. Livingston, *J. Appl. Electrochem.* 13 (1983) 429.
8. S. Biallazor, A. Lisowska-Oleksiak, *J. Appl. Electrochem.* 20 (1990) 590.
9. P.P. Kumbhar, C.D. Lokhande, *Ind. J. Chem. Technol.* 1(3) (1994) 194.
10. M.A.M. Ibrahim, *Plat. Surf. Finish.* 87(7) (2000) 67.
11. I.Z. Selim, K.M.El-Sobki, A.A. Khedr, H.M.A. Soliman, *Bull. Electrochem. Ind.* 16(7) (2000) 315.
12. H.M.A. Soliman, "*Medium Effect on Mass Transfer Coefficient in Electrodeposition Process of Copper from Acidic Copper Sulfate Solutions*", Ph.D. Thesis submitted for Faculty of Science, Alexandria University, Egypt, 1998.
13. P.K. Tikoo, V.B. Singh, S. Sultan, *Plat. Surf. Finish.* 71 (1984) 64.
14. L. Bahadur, V.B. Singh, P.K. Tikoo, *J. Electrochem. Soc.* 128 (1981) 2518.
15. H.K. Srivastava, P.K. Tikoo, *Surf. Coat. Technol.* 31 (1987) 343.
16. I.Z. Selim, A.M. Ahmed, A.A. Khedr, H.M.A. Soliman, *Bull. Electrochem. Ind.* 17(1) (2001) 27.
17. S.S. Abd El Rehim, S.M. Sayyah, M.M. El Deeb, *Appl. Surf. Sci.* 165 (2000) 249.
18. A.M. Ismail, G.A. El-Naggar, A.M. Ahmed, *Bull. Electrochem. Ind.* 17(9) (2001) 385.
19. Sh.A. El Shazly, S.S. Massoud, A.A. Zaghloul, M.T. Mohamed, M.F. Amira, *Bull. Soc. Chim.* 6 (1989) 780.
20. A.A. Taha, S.H. Sallam, A.M. Ahmed, *Anti-Corros*. 41 (1994) 10.
21. I.M. Issa, M.M. Ghoneim, A.A. El-Samahy, M. Tharwat, *Electrochim. Acta.* 17 (1972) 1251.
22. T.R. Beck, R.C. Alkire, *J. Electrochem. Soc.* 126 (1979) 1662.
23. T.C. Franklin, T. Williams, T.S.N. Narayan, R. Guhl, G. Hair, *J. Electrochem. Soc.* 144 (1997) 3064.
24. D.R. Gabe, G.D. Wilcox, *J. Appl. Electrochem.*, 28 (1998) 759.
25. M. Eisenberg, C.W. Tobias, C.R. Wilke, *J. Electrochem. Soc.* 102 (1955) 415.
26. D. Pickett, *Electrochemical Reactor Design*, Elsevier, Amsterdam 1977, 110.
27. A.M. Nasser, O.A. Fadalli, G.H. Sedahmed, *Metallkde* 80(1) (1989) 60.
28. H.A. Abdel-Rahman, "*Kinetic Studies of Cementation of Copper on Rotating Zinc Cylinder in Aqueous and Mixed Solvents*", Ph.D. Thesis submitted for Faculty of Science, Alexandria University, Egypt 1998.
29. D. Pletcher, F.C. Walsh, *Industrial Electrochemistry*, Chapman and Hall 1989, 216.
30. D.R. Russev, *J. Appl. Electrochem.* 11 (1981) 177.
31. R. Walker, S.J. Duncan, *Surf. Coat. Technol.* 27 (1986) 137.
32. G.A. Hope, G.M. Brown, D.P. Schweinsberg, K. Shimizu, K. Kobayashi, *J. Appl. Electrochem.*, Short Communication, 25 (1995) 890.
33. *Natl. Bur. Stand.* (U.S.) Circ.539 (1953) l 15.